

Holocene methane pockmarks in the Baltic Sea, Part I: Archaeal community composition based on tetraether lipids and 16S rRNA analysis

Izabela De Mey-Śnieżyńska^{1*}, Mirosław Słowakiewicz¹, Francien Peterse², Aleksandra Brodecka-Goluch⁴, Andrzej Borkowski³, Katarzyna Łukawska-Matuszewska⁴

¹University of Warsaw, Faculty of Geology, 02-089 Warsaw, Poland

²Utrecht University, Department of Earth Sciences, 3584 CS Utrecht, The Netherlands

³AGH University of Krakow, Faculty of Geology, Geophysics and Environmental Protection, 30-059 Kraków, Poland

⁴University of Gdańsk, Faculty of Oceanography and Geography, 81-379 Gdynia, Poland

*Corresponding author: i.sniezynska@uw.edu.pl

Table S1. Characterisation of the core sampling stations (P – methane-pockmark sediments; S – non-pockmark sites).

Station (polygon) ID	Latitude [N]	Longitude [E]	Water depth [m]	Submarine groundwater discharge (SGD) and methane presence	Description of the site
P/MET1-MP	54°34'	19°10'	80	Active methane-pockmark with SGD.	One of the largest pockmarks. The infiltration of freshwater characterises it. Emits gas.
S/MET1-MP			78	Non-pockmark site with very subtle SGD (based on Cl ⁻ profiles; data from unpublished cruise reports, 2017-2024).	Gas is present in the sediment, but without gas emission into the water column.
P/MET1-BH			88	Active methane-pockmark with SGD.	The deepest gas-emitting structure observed in the Baltic Sea to date (with a depth of 10 m and a diameter of 50 m). This heavily gas-charged pockmark discharged a significant volume of freshwater until mid-2019. During the latter part of 2019, an influx of saltwater from the Denmark Strait occurred, causing the freshwater layer to now lie deeper beneath the seafloor.
S/MET1-BH			79	Non-pockmark site with very subtle SGD (based on Cl ⁻ profiles; data from unpublished cruise reports, 2017-2024).	Gas is present in the sediment, but without gas emission into the water column.
P/MET3	54°44'	19°11'	97	Inactive methane-pockmark with low methane presence; no SGD.	Elongated sub-bottom furrow with shallow gas.

S/MET3			95	Non-pockmark site without SGD.	Gas is present in the sediment, but without gas emission into the water column.
P/MET4	55°07'	19°00'	104	Active methane-pockmark with subtle SGD.	The deepest pockmark in the polygon MET4.
S/MET4			99	Non-pockmark site without SGD.	Gas is present in the sediment, but without gas emission into the water column.

Validation of LOI-derived TOC (1:1 comparison)

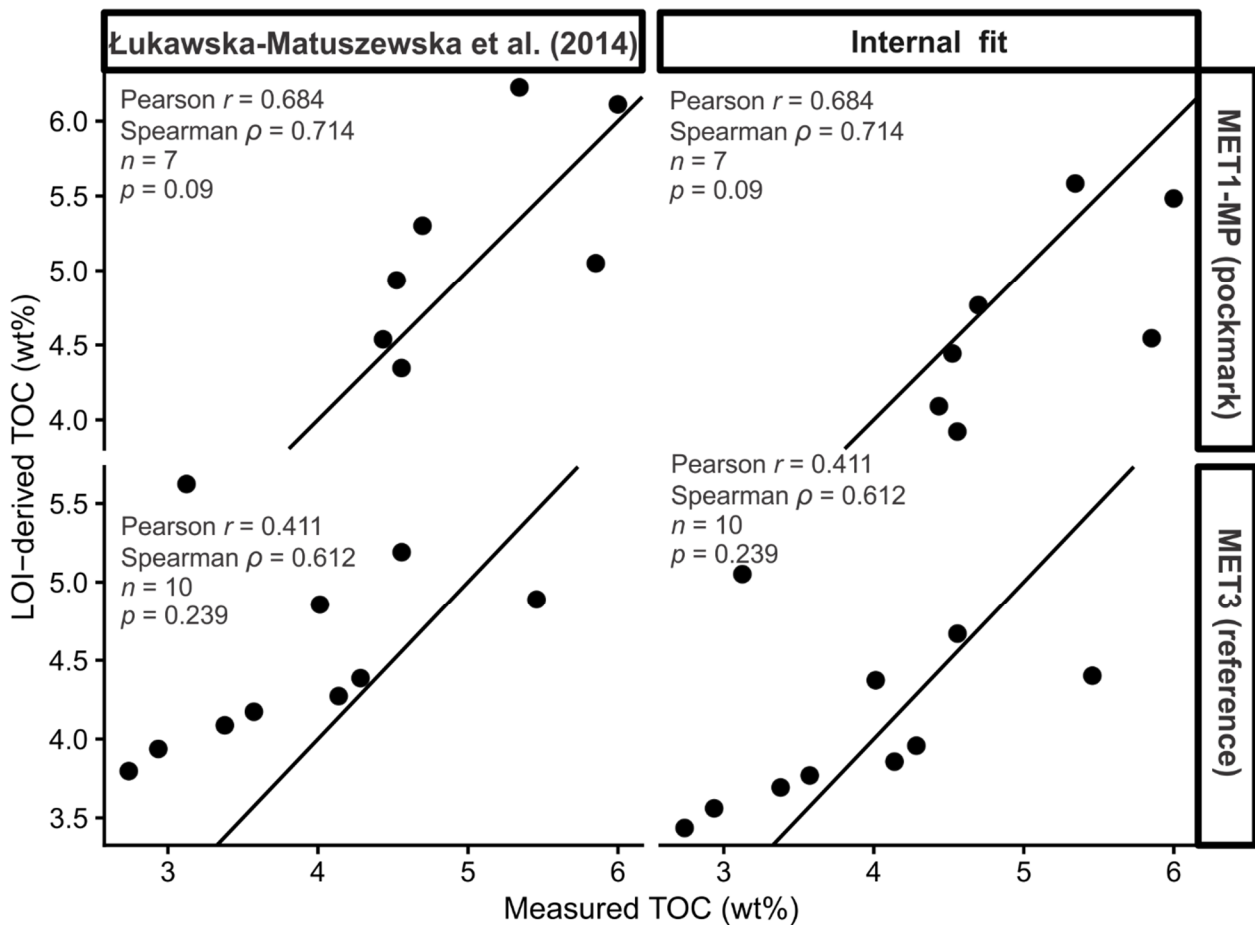


Fig. S1. Validation of LOI-derived TOC (wt%) against directly measured TOC (wt%) for cores MET1-MP (pockmark) and MET3 (reference), for both sediment types, using two LOI-TOC conversions (Łukawska-Matuszewska et al., 2014, and an internal fit based on two samples with measured TOC). The 1:1 line indicates perfect agreement; points above or below the line indicate over- or underestimation of TOC by the LOI-based approach. Pearson's r , Spearman's ρ , sample size (n), and p -values are shown for each panel.

Bland-Altman: bias and limits of agreement

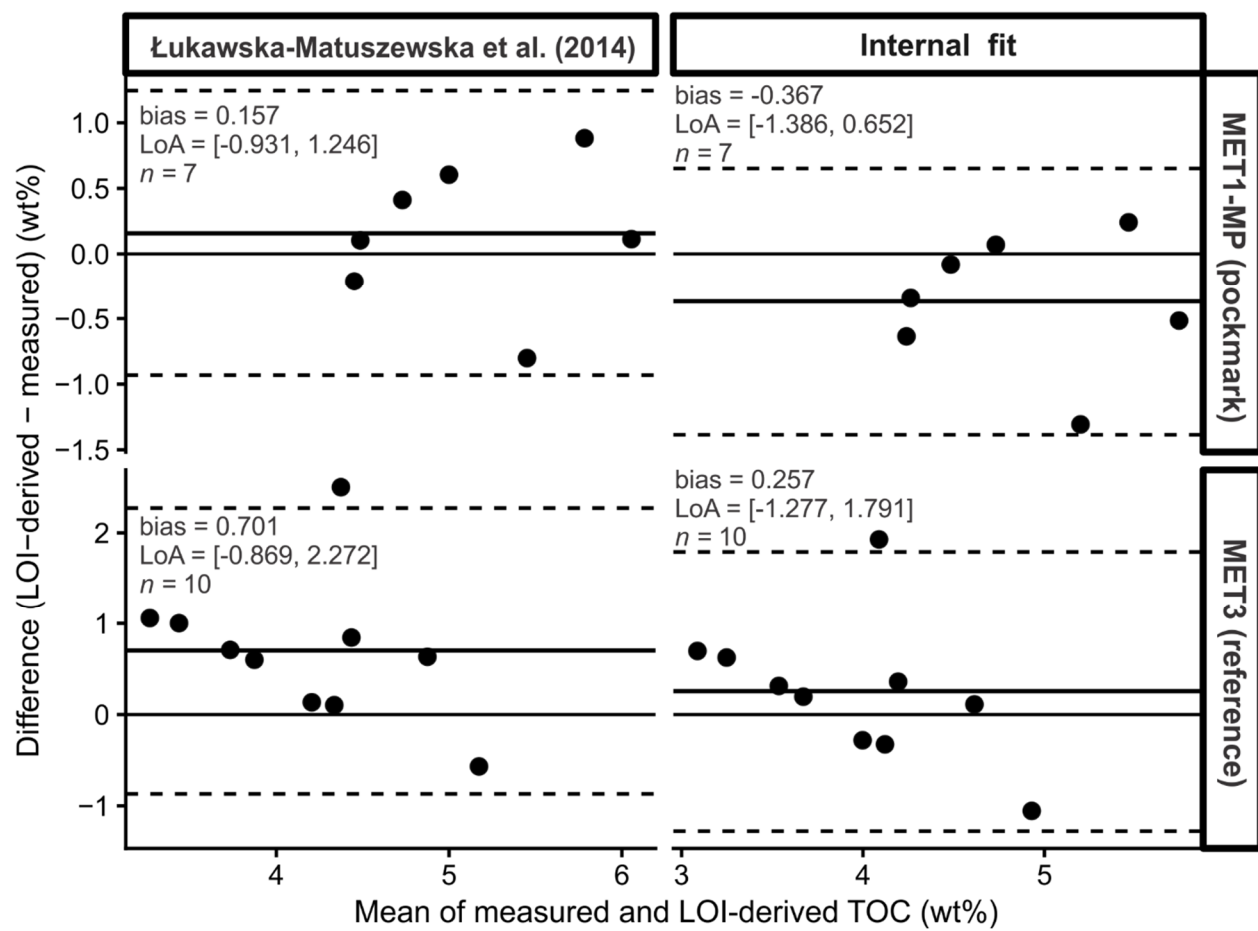


Fig. S2. Bland-Altman agreement plots comparing LOI-derived TOC with directly measured TOC. The x-axis shows the mean of the two methods, and the y-axis shows the difference ($\text{TOC}_{\text{LOI}} - \text{TOC}_{\text{measured}}$). The solid bias line represents the mean difference (systematic offset), while the dashed lines show the limits of agreement ($\text{bias} \pm 1.96 \times \text{SD}$), describing the typical range of disagreement between the two methods. LoA – limits of agreement; SD – standard deviation.

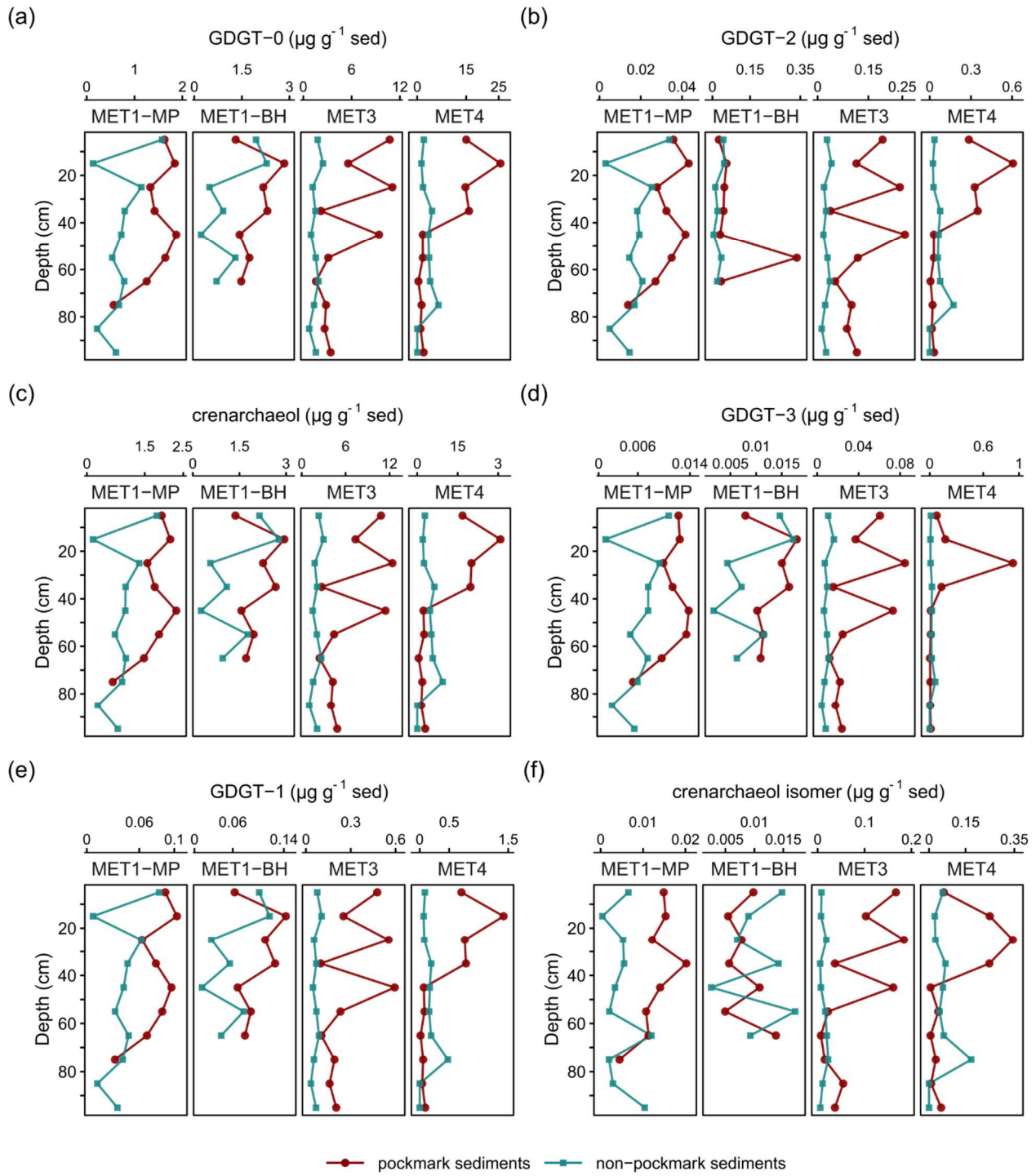


Fig. S3. Downcore variation of archaeal lipid biomarkers (a–f): iGDGTs (GDGT-0–3, cren, cren') in sediment cores collected from the Gulf of Gdańsk (MET1-MP, MET1-BH) and the Gdańsk Deep (MET3, MET4), south-eastern Baltic Sea. Concentrations ($\mu\text{g g}^{-1}$ sediment) are plotted against depth (cm). In all cores, GDGT-0 and crenarchaeol dominate the iGDGT pool, whereas GDGT-1–3 and cren' occur at lower concentrations and show more variable downcore profiles. Pockmark sediments generally exhibit elevated biomarker concentrations relative to reference sediments, with the strongest enrichments observed in the Gdańsk Deep cores.

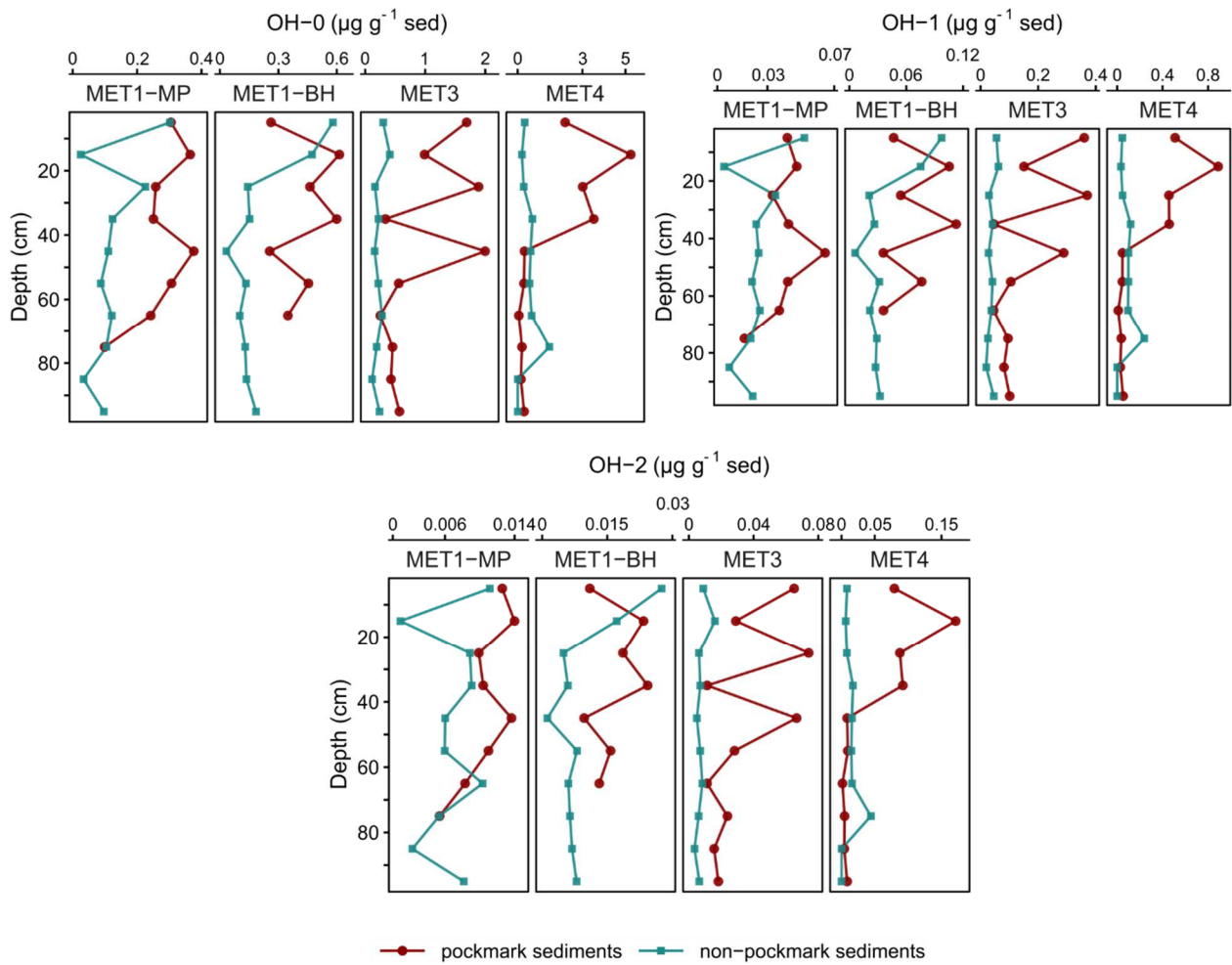


Fig. S4. Downcore variations of archaeal lipid biomarkers (OH-GDGT-0–2; $\mu\text{g g}^{-1}$ sediment) in sediment cores collected from the Gulf of Gdańsk (MET1-MP, MET1-BH) and the Gdańsk Deep (MET3, MET4), south-eastern Baltic Sea. Concentrations ($\mu\text{g g}^{-1}$ sediment) are plotted against depth (cm). OH-GDGT-0 is the predominant compound, with lower contributions from OH-GDGT-1 and OH-GDGT-2. The profiles show distinct downcore variability, with generally higher concentrations in pockmark sediments.

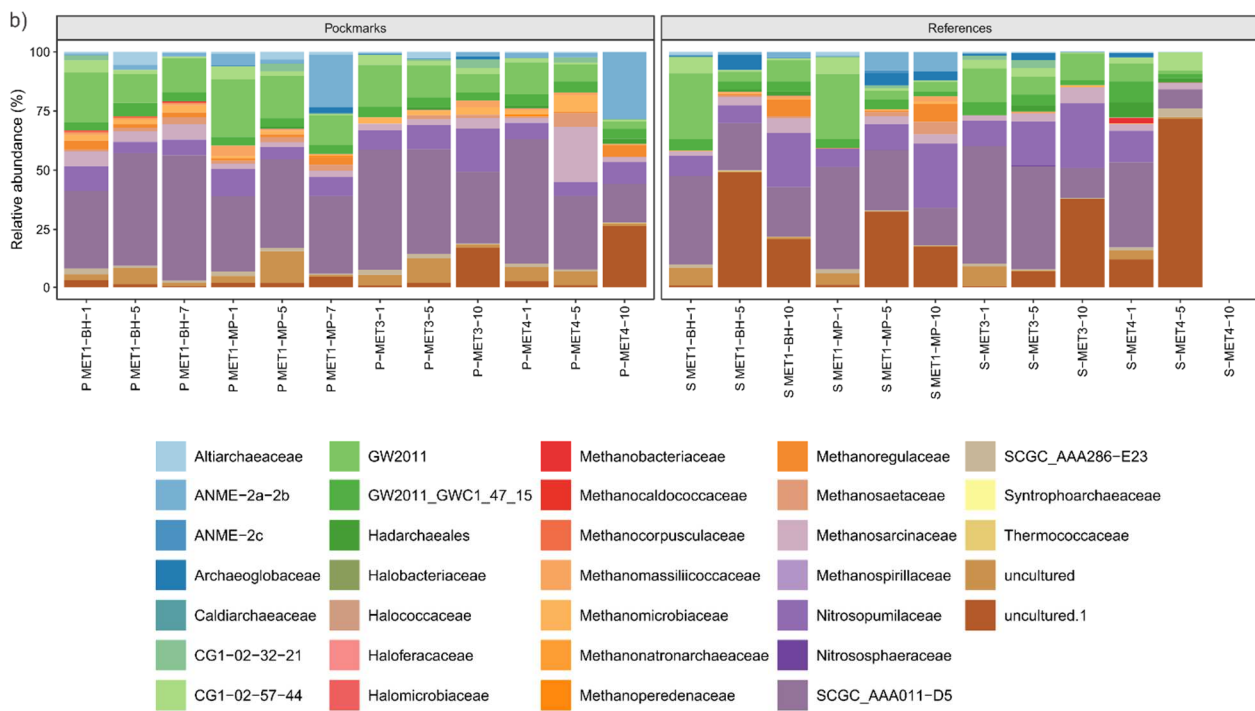
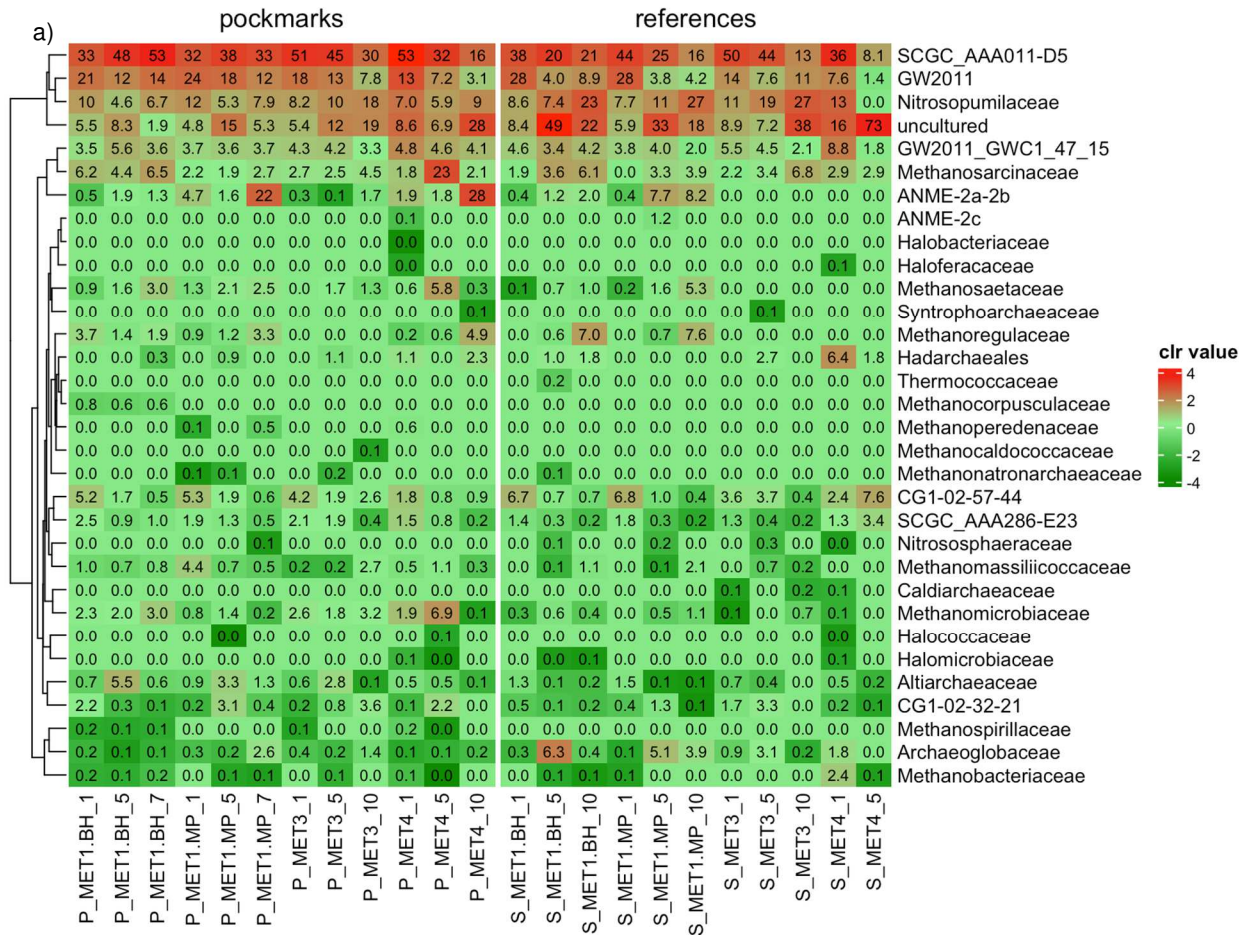
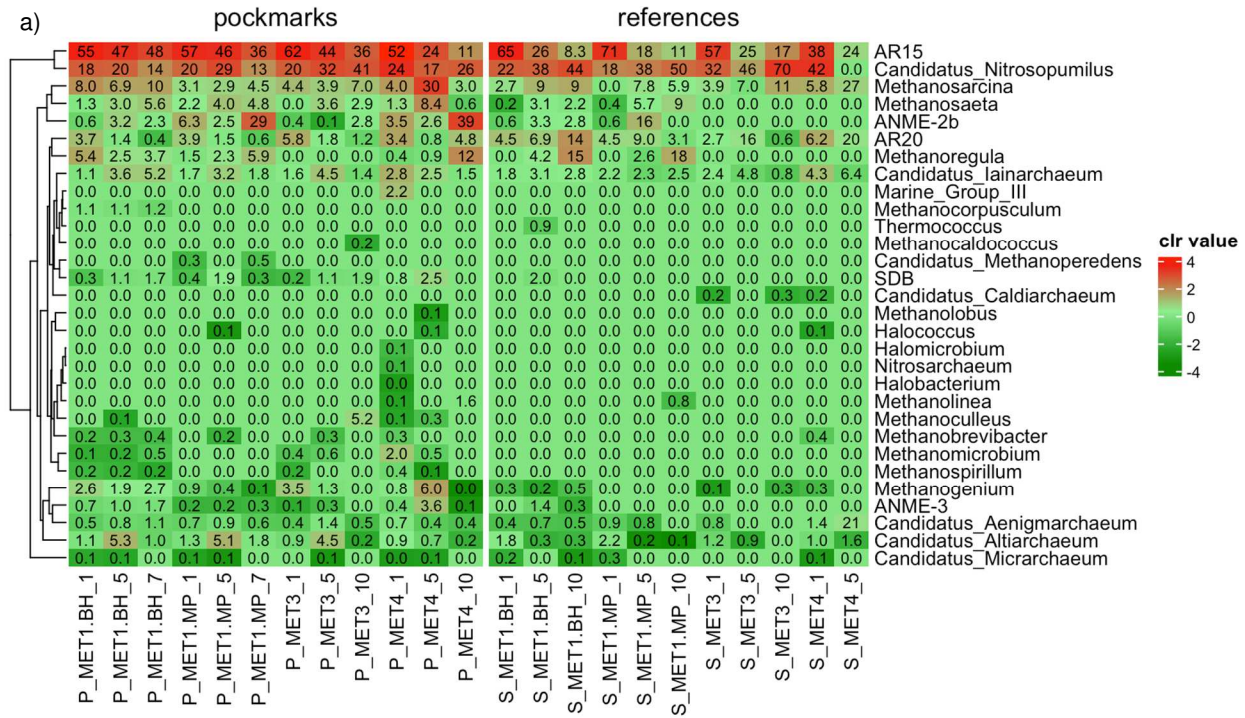


Fig. S5. (a) Heatmap of archaeal family distributions across pockmark and reference sediment samples. Rows represent archaeal families, and columns represent individual samples grouped by site type (pockmarks and references) and depth horizon at the study locations (MET1-BH, MET1-MP, MET3, MET4). Colour intensity corresponds to centred log-ratio (CLR)-transformed relative abundances, with red indicating higher and green lower relative enrichment. Hierarchical clustering of families (left dendrogram) highlights patterns of co-occurrence and differential distribution between environments. (b) Family-level composition of archaeal communities in pockmark and reference sediments. Stacked bar plots show the relative abundance (%) of archaeal families in each sample, grouped by site type (pockmarks and references) and depth interval within each study location (MET1-BH, MET1-MP, MET3, MET4). Only families with relative abundances above a defined threshold (five reads) are shown.



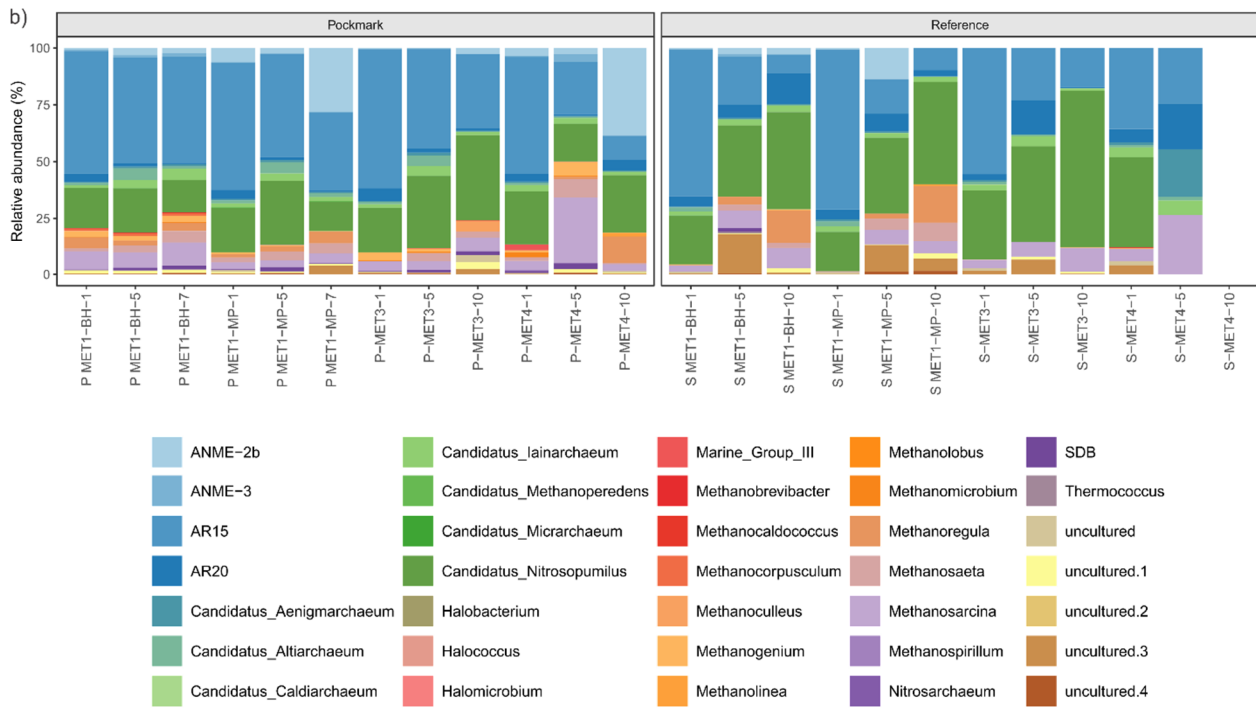


Fig. S6. (a) Heatmap of archaeal genus-level distributions across pockmark and reference sediment samples. Rows represent archaeal genera (and selected uncultured lineages), and columns represent individual samples grouped by site type (pockmarks and references) and depth horizon at the study locations (MET1-BH, MET1-MP, MET3, MET4). Colour intensity corresponds to centred log-ratio (CLR)-transformed relative abundances, with red indicating higher and green indicating lower relative enrichment. Hierarchical clustering of genera (left dendrogram) highlights patterns of co-occurrence and differential distribution between environments. (b) Genus-level composition of archaeal communities in pockmark and reference sediments. Stacked bar plots show the relative abundance (%) of archaeal genera in each sample, grouped by site type (pockmarks and references) and depth interval within each study location (MET1-BH, MET1-MP, MET3, MET4). Only genera exceeding a defined threshold (five reads) are shown.

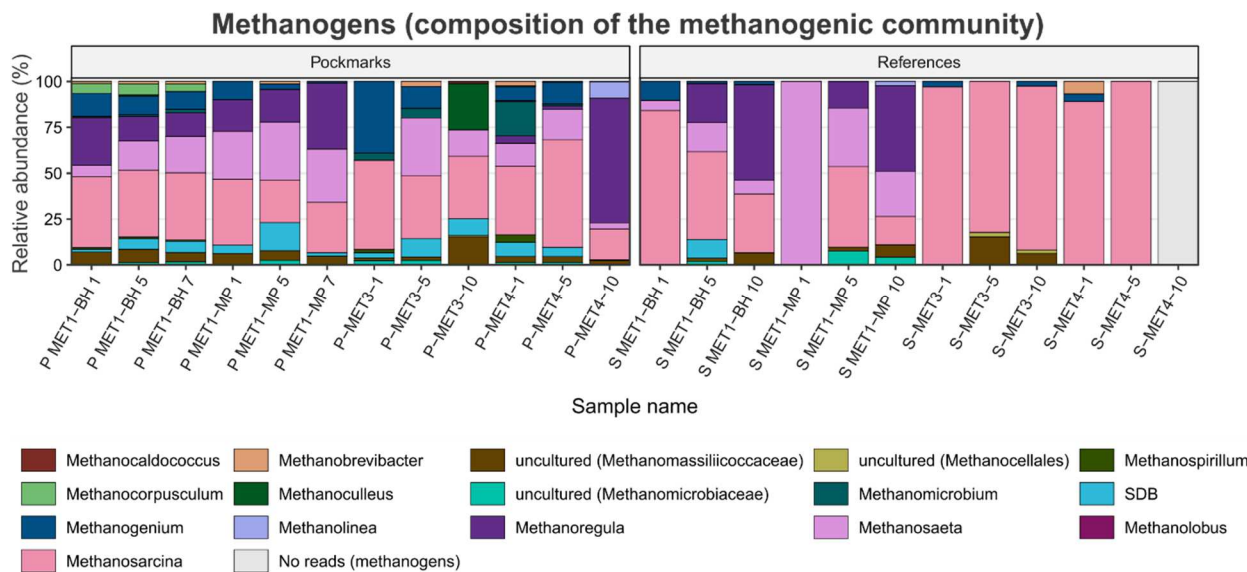


Fig. S7. Relative abundance of methanogenic archaea at the genus level in pockmark and reference sediment samples. Bars show the proportional contribution of methanogenic taxa within each sample's methanogenic community. Colours correspond to the genera shown in the legend; uncultured lineages are annotated by their lowest resolved rank (family or order). Grey bars indicate samples in which no methanogen reads were detected.

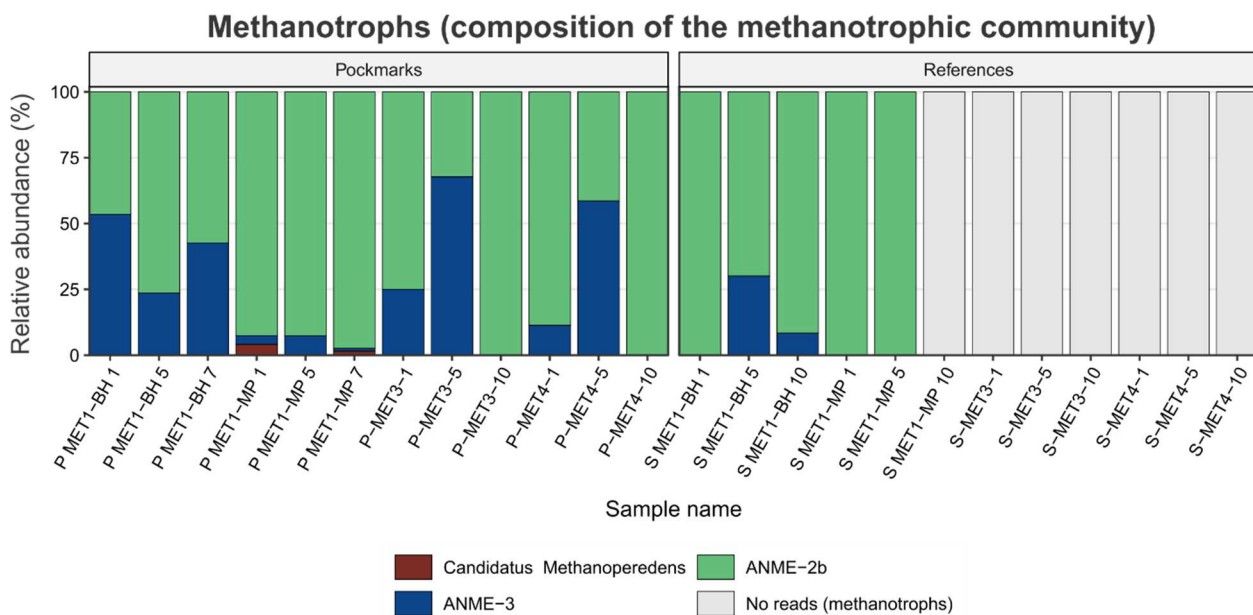


Fig. S8. Relative abundance of methanotrophic archaeal groups in pockmark and reference sediment samples. Bars show the proportional contribution of methanotroph taxa calculated within the methanotroph community of each sample. Colours indicate ANME-2b, ANME-3, and *Candidatus Methanoperedens*; grey bars denote samples with no detected methanotroph reads. ANME-1 was not detected in any of the analysed samples.

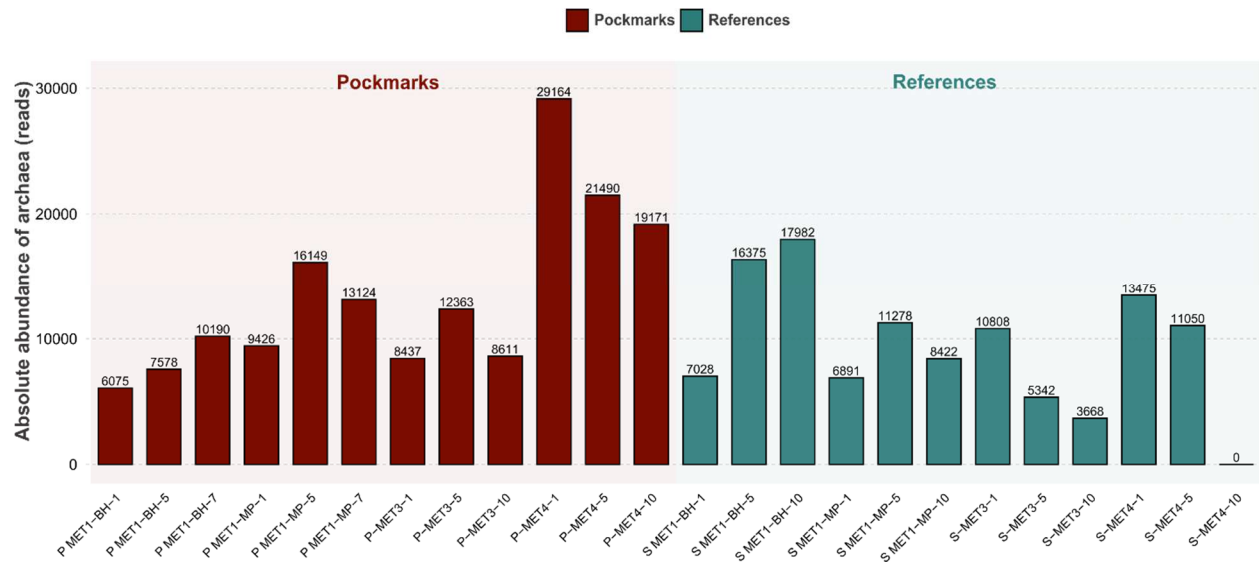


Fig. S9. Absolute abundance of archaea (reads) in pockmark and reference sediments at distinct depth horizons (surface denoted as 1; mid-depth as 5; bottom as 7 and 10).

References

Łukawska-Matuszewska, K., Kiełczewska, J., Bolałek, J., 2014. Factors controlling spatial distributions and relationships of carbon, nitrogen, phosphorus and sulphur in sediments of the stratified and eutrophic Gulf of Gdańsk. *Continental Shelf Research* 85, 168–180. <https://doi.org/10.1016/j.csr.2014.06.010>